



A long hard look on multiwavelength properties of blazar OJ 287

S. Fatima¹ · P.M.K. Anam² · K. Vierdayanti^{1,3}

Received: 15 September 2020 / Accepted: 27 March 2021 / Published online: 8 April 2021
© The Author(s), under exclusive licence to Springer Nature B.V. 2021

Abstract We examined the behaviour of blazar OJ 287 based on 12 year observation data in optic, UV, X-ray, and gamma ray. The optical, UV, and X-ray data of OJ 287 were obtained from *Swift* archive, which provide more or less simultaneous optical–X-ray observations, while gamma ray data were obtained from *Fermi* archive. The occurrence of outburst episode in 2007 can be confirmed in *Swift*/UVOT data. In addition, episodes of significant brightening (possibly the outburst(s) of this decade) can also be seen in 2015–2016 and 2016–2017. Long-term flux variability in gamma ray and X-ray data is not always concurrent with those of optical and UV. Interestingly, the high peaks appeared almost simultaneous in optic, UV and X-ray in the episode of brightening in 2016–2017. X-ray spectral fittings show that non-thermal process predominates most of the X-ray spectra. Simultaneous optical–X-ray spectral fittings show the spectral evolution and suggest the combination of thermal and non-thermal component before brightening episode in 2015–2016. We obtained gamma ray spectra with broader peak at rather high frequency compared to that expected from simple synchrotron self-Compton mechanism.

During brightening 2016–2017, the optical–X-ray fluxes are higher compared to those other periods. The shape of the X-ray and gamma ray spectra also have inverted trend than those of other periods.

Keywords BL Lacertae objects: individual: OJ 287 · Black hole physics · Accretion · Jets

1 Introduction

OJ 287 is a well-known BL Lac object which is classified as low-power blazar at redshift, $z = 0.306$ (Sitko and Junkkariinen 1985). It has been intensively studied since 1980s, when it was first suspected to have periodic optical outbursts (Sillanpää et al. 1985). The light curve during the outburst in 1983 shows similar pattern when compared to the observation in 1972 during an episode of an increasing flux (Sillanpää et al. 1985).

Analysis of historical light curve suggests the existence of periodic outburst at approximately 12 year interval and double-peaked feature in each outburst episode (Sillanpää et al. 1988; Sillanpää et al. 1996). The subsequent outburst with double-peaked feature was observed in 1994–1995 (Sillanpää et al. 1996). The unique double-peaked feature in each nearly periodic outburst episode can be explained by a model of precessing binary supermassive black holes (binary SMBHs) (e.g. Lehto and Valtonen (1996), Valtonen (2007)). In this model, the less massive SMBH (called minor SMBH) is pictured to orbit the more massive SMBH (called major SMBH). The orbit of the minor SMBH has to be quite eccentric, $e \sim 0.7$ to establish a precession rate of 39.1° per cycle (e.g. Valtonen and Lehto (1997), Valtonen (2007)). During its orbit, the minor SMBH is pictured to pass through

✉ S. Fatima
fatimas61@yahoo.com

P.M.K. Anam
pmutmainah@gmail.com

K. Vierdayanti
kiki@as.itb.ac.id

- 1 Astronomy Research Division, Faculty of Mathematics and Natural Sciences, Institut Teknologi Bandung, Bandung, Indonesia
- 2 Astronomy Study Program, Faculty of Mathematics and Natural Sciences, Institut Teknologi Bandung, Bandung, Indonesia
- 3 Bosscha Observatory, Faculty of Mathematics and Natural Sciences, Institut Teknologi Bandung, Lembang, Indonesia

the accretion disc of the major SMBH twice, before and after periastron passage. According to this model, the mass of major and minor SMBH are $(1.83 \pm 0.01) \times 10^{10} M_{\odot}$ and $(1.5 \pm 0.1) \times 10^8 M_{\odot}$, respectively, and the spin of the major SMBH was also determined to be 0.313 ± 0.01 (Valtonen et al. 2016).

Being classified as Blazar, we expect that synchrotron and synchrotron self-Compton emissions predominate the multiwavelength spectral energy distribution (SED) of OJ 287 during the non-outburst episodes when the radiation mainly comes from the jets. While during outburst, other spectral components are expected, on top of that which comes from the jets. For example, thermal bremsstrahlung process was suggested (e.g. Lehto and Valtonen (1996), Ivanov et al. (1998), Valtonen et al. (2006a), Valtonen and Sillanpää (2011)) to be detected as the minor SMBH passes through the accretion disc of the major SMBH, since the minor SMBH will cause giant gas outflow from the disc of major SMBH as it passes through. After the gas became optically thin, the gas cools off by emitting thermal bremsstrahlung radiation.

Perturbation caused by the minor SMBH as it approaches the disc of the major SMBH can also trigger additional supply of material to the jet and the non-thermal radiation will be enhanced which should appear in the spectra. Analysis of VLBA data (Britzen et al. 2018), however, found an evidence of jet precession in OJ 287 with a timescale of 24 ± 2 yr. Half of this timescale is remarkably similar to the outburst interval in optical observation. Britzen et al. (2018) argued that despite the necessity of binary SMBH to explain the jet precession (which is thought as a result of Lens-Thirring precession), the perturbation of the disc due to minor SMBH is not necessary to explain the outburst interval.

Investigation of the long-term behaviour of OJ 287 will provide a more comprehensive picture of the physical processes during outburst episodes as well as non-outburst period. While many studies of OJ 287 focused on observations during outburst period (e.g. Kushwaha (2020)), we here took a long, hard look at the behaviour of OJ 287 based on 12 year observation data in optic, UV, X-ray, and gamma ray by using *Swift*/UVOT, *Swift*/XRT, and *Fermi*/LAT data. We aim to describe the physical processes behind the long-term behaviour of OJ 287, in particular those occurring in jets and accretion disc of the major SMBH, under the assumption of the validity of precessing binary SMBH model. We will also compare our results with similar work using *Swift* data such as Siejkowski and Wiercholska (2017). In Sect. 2, we describe our data selections and methods. The main results are described in Sect. 3, focusing on the spectral analysis. In Sect. 4, we discuss our results in the context of precessing binary SMBH model and other relevant works. We conclude our work in Sect. 5.

2 Data processing and analysis tools

2.1 *Fermi* data

The gamma ray data used in this work were taken from LAT instrument of *Fermi* from 2008 to 2017. *Fermi*/LAT operates mainly in survey mode and covers a wide energy range. We followed standard data processing of *Fermi*/LAT for binned likelihood analysis of PASS 8 reconstruction event using `Fermitools 1.0.0`. The ROI used is 15° with OJ 287 coordinate as its center. Its 2.4 sr wide field of view, and large PSF at low energy, render it more complex for analysing the data. The contribution of photons from other objects outside of ROI is calculated by modelling the spectrum of each object. Therefore, the spectrum of each object in a 25° radius centered on OJ 287 is modelled according to the 3FGL catalog while, the OJ 287 spectrum is modelled by the LOGPARABOLA model. In addition, the models for galactic diffuse emission and extragalactic isotropic diffuse emission are chosen as suggested by the *Fermi*/LAT team for point source.

Fermi/LAT data are further classified into 7 periods (Period 4 to 10 in Table 1 since there is no *Fermi* data for Period 1 to 3) which correspond to brightening episodes and normal period as found from *Swift* data (see Sect. 2.2). *Fermi*/LAT data is processed in two stages. The first stage is processing data in each period with an energy range from 100 MeV to 500 GeV and the fitting parameters (normalization, α , β , and E_b) are left as free parameters. The second stage is re-processing data with shorter energy range. The energy range in first stage is divided into six parts, i.e. 100–300 MeV, 300–1000 MeV, 1–3 GeV, 3–10 GeV, 10–100 GeV, and 100–300 GeV. Three fitting parameters, i.e. α , β , and E_b of each energy range in each period are fixed to the values obtained from the first stage. While, the normalization is left as free fitting parameter for each energy range. Thus, we obtained 6 points of gamma ray flux for each period. The corresponding gamma ray energy for each range is obtained using $E_{\text{corr}} = \sqrt{E_1 \times E_2}$.

2.2 *Swift* data

2.2.1 *Swift*/XRT data

We used HEASOFT 6.16 package with CALDB 1.0.2 to process the data from *Swift*/XRT and *Swift*/UVOT. However, the *Swift*/XRT light curve was obtained using on-line *Swift*/XRT data product builder (Evans et al. 2007, 2009). We downloaded the light curve with snapshots binning for both photon counting (PC) and windowed timing (WT) modes.

The X-ray spectra were produced for each ObsID from photon counting (PC) mode only with source and background radii of 20 pixels and 50 pixels, respectively. The

Table 1 Start and end date of observation for each data group

Data group	Start–stop date	MJD	Optical light curve state	Swift RMF period
Period 1	2005/05/20–2006/12/31	53510–54100	Normal	1
Period 2	2007/01/01–2007/08/30	54101–54342	Normal	2
Period 3	2007/10/23–2007/12/21	54396–54455	2007-Outburst	3
Period 4	2007/08/31–2008/12/31 (2007-Outburst excluded)	54343–54831	Normal	3
Period 5	2009/01/01–2010/12/31	54832–55561	Normal	4
Period 6	2011/01/01–2012/12/31	55562–56292	Normal	5
Period 7	2013/01/01–2015/11/27	56293–57353	Normal	6
Period 8	2015/11/28–2016/03/28	57354–57475	Brightening 2015–2016	6
Period 9	2016/03/29–2016/10/06	57476–57667	Normal	6
Period 10	2016/10/12–2017/04/17	57673–57860	Brightening 2016–2017	6

number of used PC data are 360 ObsIDs which correspond to the observation timespan of May 2005 until January 2017. The data from *Swift*/XRT mainly has short exposure time so we did not conduct spectral analysis on each ObsID due to its low number of counts. Instead, we performed X-ray spectral analysis after co-adding several spectra which satisfied certain criteria (see for example Vierdayanti et al. (2010)). The co-added spectra must have the same Redistribution Matrix File (RMF) and similar hardness ratio.

Prior to co-adding the spectra we also grouped the spectra into brightening episodes and normal period based on the light curve profile of OJ 287 from *Swift*/UVOT. From the grouping criteria, we have 10 groups of period as shown in Table 1.

The process of co-adding spectra was conducted using MATHPHA. The corresponding Ancillary Response Files (ARFs) were also co-added using ADDARF. We only co-added spectra with signal-to-noise ratio greater than 10. The co-added spectra were further grouped to a minimum of 20 counts per bin. Spectral fittings of 0.3–10 keV energy range were carried out using several models, which are: 1) Power-law (POWERLAW); 2) Double power-law (POWERLAW+POWERLAW); 3) Disk blackbody and power-law (DISKBB+POWERLAW). Galactic absorption is fixed at $2.56 \times 10^{20} \text{cm}^{-2}$ (Kalberla et al. 2005). Since, the detail abundances in the direction of OJ 287 are not available, we used simple absorption model, i.e. WABS model.

2.2.2 *Swift*/UVOT data

The number of data from *Swift*/UVOT used in our work are 412 ObsIDs which correspond to the observation timespan of May 2005 until April 2017. All available filters were used, which are u (central $\lambda = 3465 \text{ \AA}$), b (central $\lambda = 4392 \text{ \AA}$), v (central $\lambda = 5468 \text{ \AA}$), uvw1 (central $\lambda = 2600 \text{ \AA}$), uvm2 (central $\lambda = 2246 \text{ \AA}$) and uvw2 (central $\lambda = 1928 \text{ \AA}$).

The source radius of $= 5''$ and background radius of $= 20''$ were used in the extraction process. In each ObsID, there may be more than one snapshot with different exposure times. Using UVOTSOURCE, we extracted the count rate from each snapshot to built light curves covering May 2005–April 2017, and the magnitude value (relative to Vega magnitude) to make the colour evolution of OJ 287. Average count rates from snapshots in one ObsID of each filter are used to create the *Swift*/UVOT light curve in Fig. 1.

We built the source and background PHA files using UVOT2PHA. Simultaneous UVOT and X-ray spectral fittings were done using XSPEC. We used two combination models in fitting process, i.e. REDDEN*POWERLAW+WABS*POWERLAW and REDDEN*zBREMSS+WABS*POWERLAW. The first POWERLAW and zBREMSS models were used for optic–UV part and the second POWERLAW models were used for X-ray part, in the spectrum. The zBREMSS model is to model bremsstrahlung spectrum with fixed redshift value, $z = 0.306$. We also fixed the second value of Γ which we got from X-ray spectra analysis described in the previous section, while REDDEN and WABS are additional components to model absorption in optic–UV and X-ray, respectively. We fixed the value of absorption in optic $E(B - V) = N_H/5.3 \times 10^{21} \text{cm}^{-2} = 0.048$ (Cardelli et al. 1989; Predehl and Schmitt 1995) and the value of X-ray absorption is again fixed at $2.56 \times 10^{20} \text{cm}^{-2}$ (Kalberla et al. 2005).

2.3 SED data

Spectral energy distribution (SED) of OJ 287 was built using *Swift*/UVOT, *Swift*/XRT and *Fermi*/LAT data. These data are classified into 7 periods as shown in Table 1 (Period 4–10). *Swift*/UVOT and *Swift*/XRT data use POWERLAW model and *Fermi*/LAT data use LOGPARABOLA model. Especially for *Swift*/UVOT data, we only select one obsID in each period which has best reduced χ^2 and complete filters.

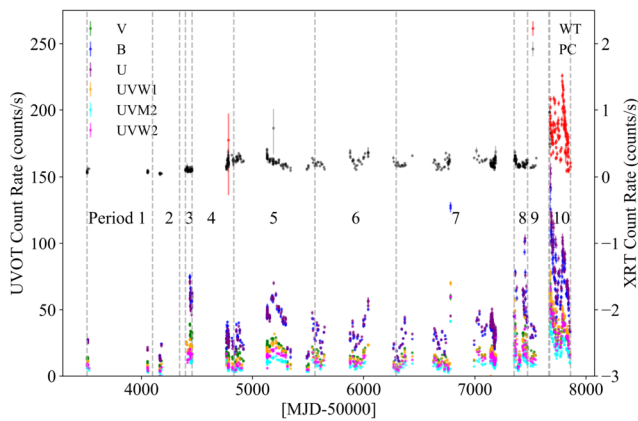


Fig. 1 UVOT and XRT light curves of OJ 287 in May 2005 - April 2017. Based on the UVOT light curves profile, there are three peaks i.e. 2007-outburst, brightening of 2015–2016 and the highest peak, brightening of 2016–2017

3 Results

3.1 Light curve

The optical, UV, and X-ray light curves are shown in Fig. 1. From optical and UV light curves, three episodes of brightening can be seen, i.e. 2007-outburst, 2015–2016 and 2016–2017. Here we do not specifically use the term “outburst” for brightening in 2015–2016 and 2016–2017 since the nature of those brightening episodes are yet to be confirmed.

From the history of OJ 287 outburst, there were 2 outburst peaks in one orbital period, the so-called double-peaked feature. The first peak was usually the highest peak observed in optical band. The brightening in 2016–2017 has higher intensity than that of 2015–2016. That is, based on the outburst history information brightening in 2016–2017 might be the first peak of the outburst in this decade while the brightening in 2015–2016 might be considered as pre-outburst brightening.

The profiles of 2005–2017 optical and UV light curves are quite similar but with different intensity. At the top of Fig. 1 we show the X-ray light curves of OJ 287 from *Swift*/XRT in WT and PC mode. We only noticed two prominent brightenings, i.e. after 2007-outburst and coincident with brightening in 2016–2017. Both outbursts were detected using WT mode. While in PC mode, only brightening in 2015–2016 was detected. We can also compare the details of optical, UV, and X-ray light curve trends in narrow interval of time. By comparing the narrow interval light curves for each filter we noticed some patterns in variability between optic–UV and X-ray. These are: 1) Similar pattern; 2) Contrary pattern, i.e. optic–UV has positive correlation but optic–X-ray or UV–X-ray has negative correlation, and vice versa; 3) Delay pattern. Note, however, this finding was not based on quantitative analysis.

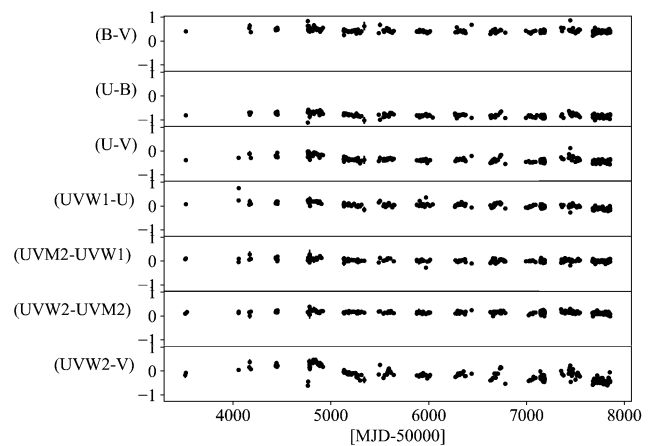


Fig. 2 Colour evolution of OJ 287 in May 2005 - April 2017. The colour evolution made in the seven scenarios (B–V), (U–B), (U–V), (UVM1–U), (UVM2–UVM1), (UVW2–UVM2), (UVW2–V)

The intensity of 2007-outburst ($54396 \leq MJD \leq 54455$) was smaller than the intensity of brightening in 2015–2016 ($57354 \leq MJD \leq 57475$) and 2016–2017 ($57673 \leq MJD \leq 57860$). This may be related to the 60 years modulation period due to precession effect (Lehto and Valtonen 1996; Valtonen et al. 2006a). At the time of 2007-outburst, the X-ray light curve showed no significant increase in intensity but there was an indication of delay in X-ray, relative to those of optical and UV outbursts. An increase of X-ray intensity was detected from WT data around November 2008 ($MJD = 54782$). In fact, the X-ray intensity of OJ 287 at the time of the optical 2007-outburst was lower than its average daily intensity. In contrast to 2007-outburst, the brightening in 2016–2017 was quickly followed by the brightening in X-ray as can be detected from WT data.

We also checked colour variability between optic–optic, optic–UV and UV–UV (See Fig. 2). In general, the results show quite stable color during 2005–2017. Sillanpää et al. (1996) found the stability of V and R colour during outburst 1994 while Gupta et al. (2017) confirmed the phenomena during brightening 2015–2016 in some optical bands.

In the next subsection we will examine the spectra in these bands as well as X-ray and gamma ray to get more detailed information about the energy generation processes.

3.2 *Fermi*/LAT, *Swift*/XRT and *Swift*/UVOT spectra

The gamma ray spectra are modelled with LOGPARABOLA function. It has four fitting parameters, i.e. normalization, α , β , and E_b . The results of fitting parameters and fluxes in each period are shown in Table 2. The value of α , which indicates the slope of spectrum, fluctuates from Period 4 until 9, before significantly decreasing in Period 10 which shows the existence of curvature in the spectra at high energy region. In other words, we found the brightening episode in

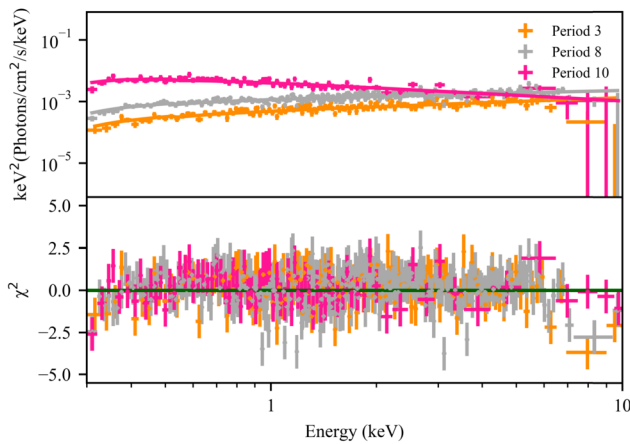


Fig. 3 *Swift*/XRT spectra of OJ 287 in brightening episodes

2016–2017 has flattened spectrum compared to those of the normal period and brightening episode in 2015–2016. The value of β significantly decreases from Period 4 to Period 5, and generally increases after Period 6, before decreasing again in Period 10. The value of E_b only changes very little in all periods. Fluxes of OJ 287 in all periods decrease from smallest to highest energy at different rates for each period.

As for the X-ray spectra, we find that double power-law model gives unrealistic values of photon index (Γ). In general, the obtained values of Γ are extreme with large error values.

We further checked if thermal component is needed in the X-ray spectra. However, in general, the additional thermal component, DISKBB is not needed statistically and in some periods it produces unrealistic results.

Moreover, the value of kT_{in} which corresponds to the inner disc temperature is $(1.83^{+0.83}_{-0.5}) \times 10^7$ K which is too high to represent the temperature of the accretion disc of SMBH. We, therefore, conclude that the best fit model for all of the X-ray spectra groups is single power-law. We have tried to replace the absorption model with TBABS and the obtained fitting results are very similar, without significant improvement in the residue of the fitting. We have also tried to make N_H as free fitting parameter and we found that in most periods, the obtained values of N_H are comparable to that of Kalberla et al. (2005). Only in period 3 and 6 that the obtained values are higher by a factor of two, which may suggest intrinsic absorption in OJ 287.

The value of photon index, Γ , and reduced χ^2 are shown in Table 3. The value of Γ varies during May 2005–October 2016 within range, $1.55 \pm 0.05 < \Gamma < 2.60 \pm 0.06$. The spectral evolution can be found in Fig. 3, for 2007-outburst and two brightening episodes of 2015–2016 and 2016–2017, and in Fig. 4 for normal period. We can see that spectrum of the brightening episode in 2016–2017 has the steepest slope compared to the other spectra. The value of photon index, Γ , are below 2.5 except for the brightening episode

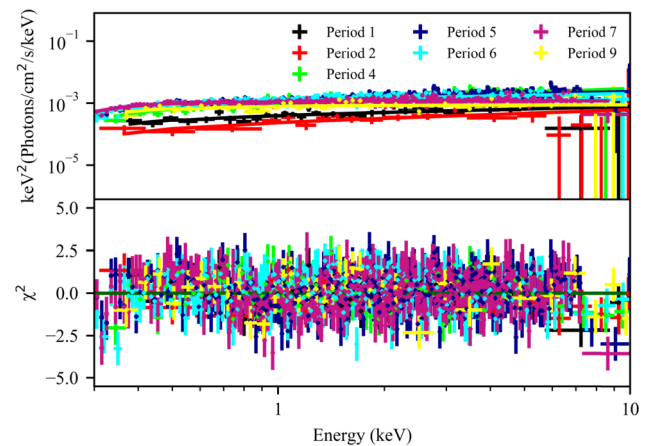


Fig. 4 *Swift*/XRT spectra of OJ 287 in normal periods

in 2016–2017. We also calculated the X-ray luminosity of the POWERLAW model during the May 2005–October 2016, the range of X-ray luminosity is $(5.17^{+0.88}_{-0.82}) \times 10^{44} < L_x < (4.99^{+0.20}_{-0.11}) \times 10^{45}$ erg s $^{-1}$.

Finally, we fitted the optical–UV–X-ray spectra from *Swift*/UVOT and *Swift*/XRT simultaneously. Not all spectra can be fitted with both models used in this simultaneous fitting described in the previous section. We summarized the number of spectra with acceptable fit for both models in Table 4. For (POWERLAW+POWERLAW) model, we got the Γ_{uvo} in range of $2.65 \pm 0.02 < \Gamma_{uvo} < 3.26^{+0.11}_{-0.14}$ for normal period and $2.88 \pm 0.02 < \Gamma_{uvo} < 4.51^{+1.23}_{-0.85}$ for the brightening episodes including the 2007-outburst. While for (ZBREMSS+POWERLAW) model we got the value of kT in range of $(2.97^{+1.0}_{-0.7}) \times 10^{-3} < kT < (5.26^{+2.06}_{-1.16}) \times 10^{-3}$ keV or equal to electron temperature of $(3.44^{+1.15}_{-0.81}) \times 10^5 < T < (6.10^{+2.39}_{-1.35}) \times 10^5$ K. Fig. 5 and Fig. 6 are examples of optical–UV–X-ray spectral modelling with (POWERLAW+POWERLAW) for brightening episodes and normal periods, respectively.

We would like to bring to the attention the number of spectra with acceptable fit for (ZBREMSS +POWERLAW) model in Period 7 and 8 as shown in Table 4. The optical–UV regions in Period 7 and 8, which correspond to the time from 1st of January 2013 until 28th of March 2016, are better fitted with thermal bremsstrahlung model. In the context of binary SMBH model, the thermal bremsstrahlung emission has been proposed as the observed emission when the minor SMBH crossed the disc of the major SMBH. In our work, however, the thermal bremsstrahlung was more pronounced in the normal period preceding the brightening episode in 2015–2016 (Period 7) and extended until the brightening episode in 2015–2016. Note that the UVOT spectra used in this fitting are essentially photometric data of several different optical and UV filters.

Table 2 Gamma ray fitting parameters of LOGPARABOLA model

Data group	Energy (GeV)	LOGPARABOLA model				Flux (10^{-8} Photons/cm ² /s)
		Normalization (10^{-11})	α	β	Eb	
Period 4	0.1–0.3	1.43 ± 0.24	2.10 ± 0.14	0.12 ± 0.05	706.53 ± 335.01	4.17 ± 0.71
	0.3–1	1.22 ± 0.14				1.44 ± 0.16
	1–3	1.08 ± 0.17				0.30 ± 0.05
	3–10	1.43 ± 0.38				0.09 ± 0.02
	10–100	0.96 ± 0.85				$(8.25 \pm 7.29) \times 10^{-3}$
	100–300	$(1 \pm 2.18) \times 10^{-4}$				$5.87 \times 10^{-9} \pm 1.28 \times 10^{-8}$
	0.1–500	1.21 ± 1.21				5.40 ± 0.70
Period 5	0.1–0.3	0.98 ± 0.08	2.24 ± 0.04	0.03 ± 0.02	706.65 ± 172.28	4.30 ± 0.33
	0.3–1	0.94 ± 0.06				1.19 ± 0.08
	1–3	0.88 ± 0.08				0.24 ± 0.02
	3–10	1.01 ± 0.15				$0.07 \pm 9.97 \times 10^{-3}$
	10–100	0.99 ± 0.31				$0.01 \pm 4.29 \times 10^{-3}$
	100–300	$(1 \pm 2.22) \times 10^{-4}$				$(3.41 \pm 7.56) \times 10^{-8}$
	0.1–500	0.93 ± 0.51				5.60 ± 0.37
Period 6	0.1–0.3	2.00 ± 0.11	2.16 ± 0.03	0.03 ± 0.01	706.60 ± 107.09	7.75 ± 0.44
	0.3–1	2.09 ± 0.08				2.56 ± 0.10
	1–3	2.03 ± 0.11				0.58 ± 0.03
	3–10	1.93 ± 0.20				0.15 ± 0.01
	10–100	2.01 ± 0.39				$0.04 \pm 7.14 \times 10^{-3}$
	100–300	2.32 ± 2.33				$(1.25 \pm 1.26) \times 10^{-3}$
	0.1–500	2.02 ± 0.66				11.09 ± 0.43
Period 7	0.1–0.3	1.74 ± 0.09	2.19 ± 0.03	0.08 ± 0.02	706.67 ± 102.18	6.39 ± 0.34
	0.3–1	1.64 ± 0.06				2.01 ± 0.08
	1–3	1.67 ± 0.09				0.45 ± 0.02
	3–10	1.63 ± 0.17				0.10 ± 0.01
	10–100	1.85 ± 0.43				$0.02 \pm 4.36 \times 10^{-3}$
	100–300	$(1 \pm 2.29) \times 10^{-4}$				$(1.27 \pm 2.90) \times 10^{-8}$
	0.1–500	1.67 ± 0.53				8.76 ± 0.33
Period 8	0.1–0.3	2.68 ± 0.28	2.18 ± 0.06	0.07 ± 0.03	706.92 ± 205.50	9.93 ± 1.04
	0.3–1	2.69 ± 0.21				3.30 ± 0.26
	1–3	2.69 ± 0.30				0.74 ± 0.08
	3–10	2.21 ± 0.54				0.14 ± 0.03
	10–100	0.45 ± 1.75				0.05 ± 0.02
	100–300	0.0019 ± 0.3803				$3.39 \times 10^{-7} \pm 6.80 \times 10^{-5}$
	0.1–500	2.72 ± 1.72				14.40 ± 1.02
Period 9	0.1–0.3	1.00 ± 0.23	2.09 ± 0.10	0.06 ± 0.04	706.68 ± 336.18	3.32 ± 0.78
	0.3–1	1.37 ± 0.14				1.63 ± 0.17
	1–3	1.05 ± 0.17				0.31 ± 0.05
	3–10	1.29 ± 0.36				0.08 ± 0.02
	10–100	1.50 ± 0.68				0.03 ± 0.01
	100–300	$1.06 \times 10^{-4} \pm 1.20 \times 10^{-2}$				$3.99 \times 10^{-8} \pm 4.54 \times 10^{-6}$
	0.1–500	1.17 ± 1.16				5.75 ± 0.74

Table 2 (Continued)

Data group	Energy (GeV)	LOGPARABOLA model				Flux (10^{-8} Photons/cm ² /s)
		Normalization (10^{-11})	α	β	Eb	
Period 10	0.1–0.3	0.92 ± 0.27	1.89 ± 0.10	0.04 ± 0.03	706.68 ± 349.39	2.38 ± 0.69
	0.3–1	1.01 ± 0.13				1.12 ± 0.14
	1–3	1.38 ± 0.16				0.49 ± 0.06
	3–10	1.15 ± 0.23				0.14 ± 0.03
	10–100	1.12 ± 0.37				0.05 ± 0.02
	100–300	$1 \times 10^{-4} \pm 2.26 \times 10^{-6}$				$1.88 \times 10^{-7} \pm 4.26 \times 10^{-9}$
	0.1–500	1.15 ± 1.07				4.82 ± 0.67

Table 3 X-ray fitting parameter of power-law model

Data group	Power-law model	
	Γ	$\chi^2/\text{d.o.f}$
Period 1	1.73 ± 0.11	32.15/252
Period 2	1.61 ± 0.17	38.49/543
Period 3	1.59 ± 0.04	163.31/337
Period 4	1.55 ± 0.05	110.66/312
Period 5	1.75 ± 0.02	326.09/431
Period 6	1.79 ± 0.03	247.49/399
Period 7	2.00 ± 0.02	354.70/370
Period 8	1.73 ± 0.03	319.47/428
Period 9	1.97 ± 0.11	57.58/484
Period 10	2.60 ± 0.06	70.61/420

Table 4 Number of spectra with acceptable fit for (POWERLAW+POWERLAW) model and (ZBREMS+POWERLAW) model

Data group	POWERLAW+ POWERLAW	ZBREMS+ POWERLAW	Total
Period 1	1	0	3
Period 2	0	0	2
Period 3	0	0	9
Period 4	3	0	11
Period 5	15	12	68
Period 6	17	3	31
Period 7	10	112	116
Period 8	21	35	39
Period 9	0	0	7
Period 10	0	0	2

3.3 SED of OJ 287

Next, we examine the full spectral energy distribution (SED) of OJ 287. In the SED of Blazar, in general (e.g. Ghisellini

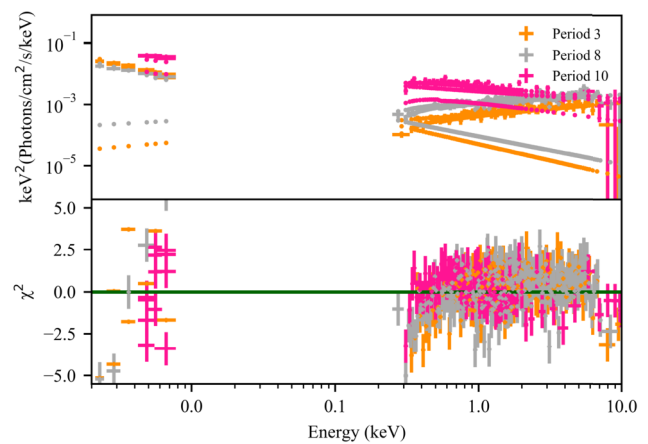


Fig. 5 *Swift*/UVOT and XRT spectra of OJ 287 in brightening episodes

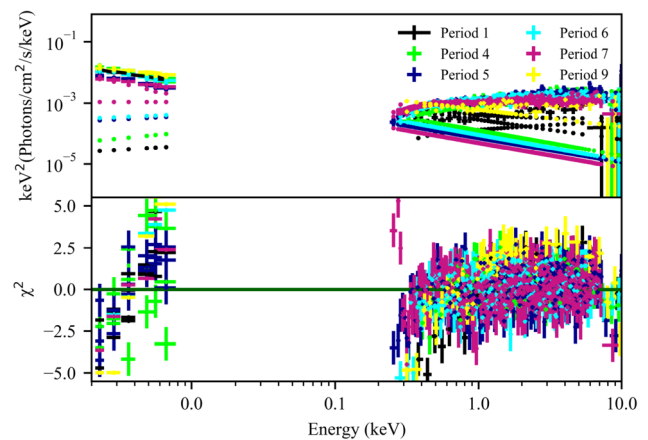


Fig. 6 *Swift*/UVOT and XRT spectra of OJ 287 in normal periods

et al. (2017)), the ascending trend for higher frequency peak in Blazar SED corresponds to the start of the synchrotron self-Compton component. We can see, however, in Fig. 7 that the SED of the brightening episode in 2016–2017 (Period 10) can be distinguished from the SEDs of other periods. The flux of UVOT data is significantly higher (a factor of about three times) than those of other periods. Moreover,

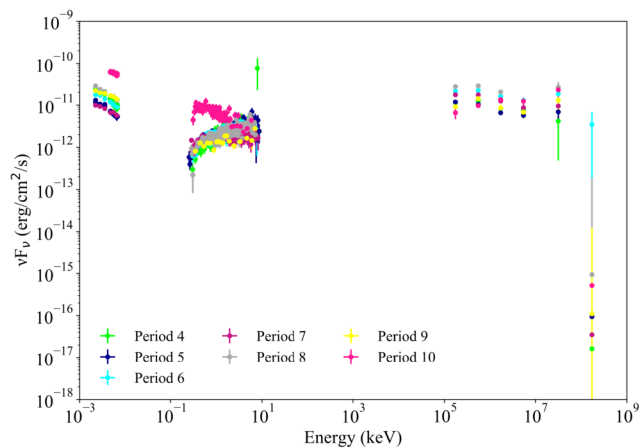


Fig. 7 SED of OJ 287 by plotting simultaneously the spectra from *Swift*/UVOT, *Swift*/XRT and *Fermi*/LAT. For spectra from *Swift*/UVOT we only choose spectra with good statistical quality and only seven periods have it. It is quite clear that brightening 2016–2017 has a different profile compared to the others. This indicates that there is a shifting in the blazar's higher peak

the X-ray data of Period 10 show declining trend while the others show ascending trend. The flux in the lowest X-ray energy is ten times higher than in the other periods. It is possible that during the brightening episode in 2016–2017, the synchrotron component extends to the X-ray energy band and the peak of synchrotron self-Compton shifts to the higher energy as well.

From the binary SMBH model, it is suggested that during the first outburst peak in the outburst optical light curve, bremsstrahlung radiation should be detected as a result of the impact of the minor SMBH to the disc of the major SMBH. However, in this work, we cannot rule out the (POWERLAW+POWERLAW) model for the brightening episode in 2016–2017. Moreover, as we previously mentioned, the thermal bremsstrahlung model is more prominent in the normal period preceding the brightening episode in 2015–2016.

Then, the higher energy peaks of all periods which are interpreted as synchrotron self-Compton radiation appear broader compared to synchrotron self-Compton model shown in Valtonen et al. (2012) and it shifts to higher energy in the brightening episode in 2016–2017. Our results of optical–X-ray data are similar to that of Valtonen et al. (2012) and our gamma ray data are also very similar to the archival data in Valtonen et al. (2012) and cannot be explained by a simple synchrotron self-Compton model.

4 Discussion

Siejkowski and Wiercholska (2017) studied OJ 287 in optic, UV and X-ray also using data from *Swift*/UVOT and *Swift*/XRT from 2005 to June 2016. They found that the

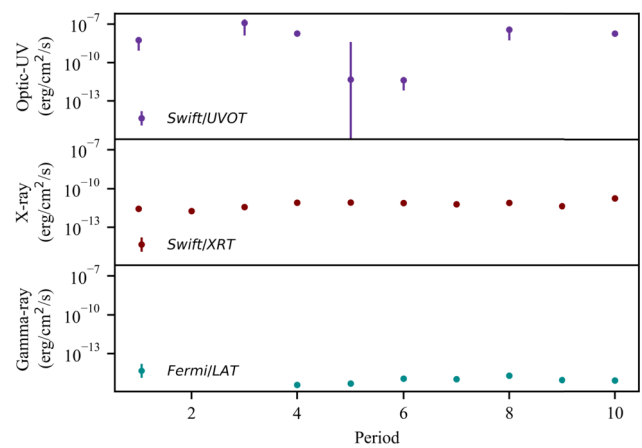


Fig. 8 Light curve per period of Optic - UV, X-ray and gamma-ray. To make light curve per periods, we also determined flux from the simultaneous spectra in range of *Swift*/UVOT energy, i.e. 2–7 eV, using command FLUX and FLUX_ERROR in XSPEC. We only choose one ObsID with the best fit model from each group of periods

shortest variability time-scale is one day. They also found that the optical and UV variability are very similar. While the variability pattern between optic-UV and X-ray is not correlated. Kushwaha et al. (2018) studied the detail of the brightening of 2016–2017. They found that an outburst in X-ray occurred coincidentally with the optical–UV outburst but they could not find significant change in the gamma ray light curve. Even though in our work timing analysis is not yet done, we confirmed the results of Siejkowski and Wiercholska (2017) in terms of the similarity between optical and UV variability. We also confirmed that long-term flux variability in X-ray data is not always concurrent with those of optical and UV. In some cases, X-ray flux variability appears to be irrelevant to those of optical and UV. We also confirmed that the brightening in 2016–2017 occurred in all optic–X-ray data as reported by Kushwaha et al. (2018). On the other hand, the gamma ray flux during the brightening in 2016–2017 was not the highest flux. However, we noticed a different pattern in the gamma ray spectral profile as can be seen from Fig. 7. There is no clear correlation between optical, X-ray and gamma ray fluctuation (see Fig. 8).

In Fig. 9, we show gradual declining patterns in the optic–UV light curve similar to the ones reported in (Sillanpää et al. 1985). In (Sillanpää et al. 1985) the optical light curve was obtained during the outburst in 1983 and it was shown that the declining pattern is very similar to that of the 1972 outburst. In our work, the light curve shown in Fig. 9 is also obtained during the brightening in 2016–2017, supporting the idea that the brightening in 2016–2017 is the first peak of the outburst in this decade, while the brightening in 2015–2016 can be considered as a precursor.

The double peak is used by Valtonen (2007) as a hint to predict the outbursts time in the context of the binary

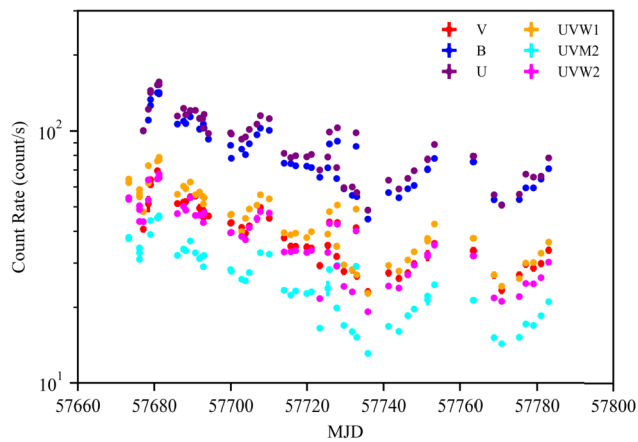


Fig. 9 Light curve of brightening 2016–2017

SMBH model with two values scenarios of precession, i.e. $37^\circ.5$ and $39^\circ.1$. From their simulation they got the prediction of outburst's time. The first outburst peak of this decade was predicted to happen in December 2015 or March 2016 for each precession scenario, respectively. And the second outburst peak for both precession scenarios was predicted to happen in around July 2019. However, from our investigation based on the long term optical - UV light curve, we got two significant brightenings, i.e. brightening in the last months of 2015 until about March of 2016 and in the last months of 2016 until around the first months of 2017. From the previous study (Sillanpää et al. 1996; Valtonen et al. 2006b) the first outburst peak always corresponds to the major brightening episode in one orbital period. Valtonen (2007) suggested that the first outburst peak corresponds to the time when minor SMBH passes through the disc. According to the model, the first outburst peak can be explained as the result of collision between minor SMBH and the accretion disc of major SMBH. As the minor SMBH moves toward the periapsis the velocity increases and the impact is greater. While the second outburst peak tends to be smaller in intensity as the minor SMBH leaves the periapsis.

In some outburst seasons, smaller intensity brightening may be detected prior to the first outburst peak (Valtonen et al. 2006a). This brightening might be caused by disruption of the major SMBH accretion disc by minor SMBH even before the impact (Valtonen et al. 2006a). The lower intensity brightening in 2015–2016 found in *Swift*/UVOT and XRT data may be an evidence of such brightening.

However, there are some contradicting findings. Valtonen et al. (2017) reported the polarization degree (PD) at the time of the brightening in 2015 is very low, i.e. the value of PD is 0.1 or below. The low PD indicates that the brightening is caused by thermal bremsstrahlung process after minor SMBH's dive into the accretion disc of major SMBH. As a matter of fact, we also got the evidence of significant bremsstrahlung radiation in the optic - UV

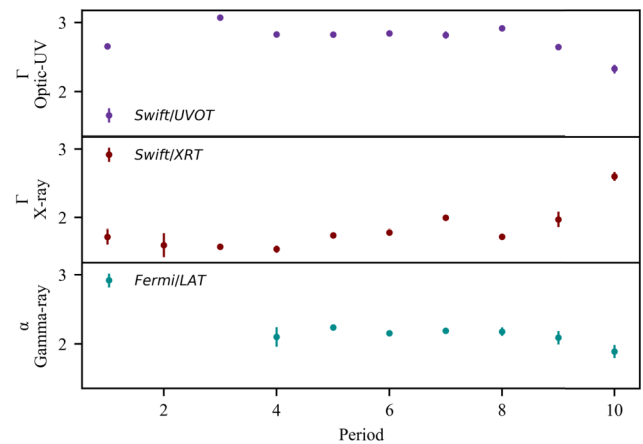


Fig. 10 Best fit Parameter of spectra form *Swift*/UVOT, *Swift*/XRT and *Fermi*/LAT. Interestingly, the Γ of X-ray spectra have anti-correlated with α of gamma ray spectra

regimes during 2013–2015. Spitzer observation reported a detection of a brightening during July - September 2019 and the flux behaviour has strong similarity with outburst in September 2007 (Laine et al. 2020). There were also some report on the occurrence of the brightening in X-ray detected by *Swift*/XRT around January 2019 and in gamma ray detected by *Fermi*/LAT around July 2019 (MJD 58780). The brightening episode in mid 2019 reported by several missions above match the prediction of the second outburst time by Valtonen (2007).

We also studied the spectral evolution of OJ 287 in X-ray since 2005 until 2017 by using co-added *Swift*/XRT spectra. We found that the X-ray spectral shape is quite similar for all of periods, except period 10. Siejkowski and Wiercholska (2017) found that the harder the optical - UV spectra, the softer the X-ray spectra become. In our investigation we found the steeper the photon index of optic - UV spectra, the flatter the photon index of X-ray spectra become (see Fig. 10). The photon index of gamma ray spectra do not change as much except for group 10, i.e. in time of brightening of 2016–2017. During 2005–2017, it was reported that the highest flux observed in gamma ray by Veritas was during the brightening in 2016–2017 (O'Brien 2017).

Siejkowski and Wiercholska (2017) also found that there were flat X-ray spectra around January until June 2015 after which the spectra returned to the previous trend. They proposed two scenarios, i.e. an overlap of two Blazar spectral components and a new additional component in X-ray regime. It seems like SED of OJ 287 is affected by attractive interaction between both SMBHs which results in periodic nature. Shifting of the SED happened at the time of brightening of 2016–2017. Although Kushwaha et al. (2018) noticed the existence of inverted spectra since around middle of June 2016, they found that the stable state of inverted spectra happened since 16th of October 2016 (MJD = 57552) until 28th of March 2017 (MJD = 57840) with steep values

of the X-ray spectral index (2.5 – 3). In our work, we also found, during 2016–2017 brightening, that the X-ray spectra has inverse trend and steep photon index (> 2.5) compared to other X-ray spectra of the previous periods since 2005. These unique features appear to be a new puzzle of OJ 287 energy generation mechanism. Kushwaha (2020) explained that the source of the energy in MeV–GeV during outburst of 2016–2017 as external Comptonization (EC) which produce very huge energy which cause the shifting of the high energy peak to higher energy in the SED.

In general, being a blazar, the SED of OJ 287 is presumed to be dominated by the non-thermal processes occurring in the jets. Synchrotron radiation is usually considered as the main component of the first peak of the SED. On the other hands, the non-thermal process responsible for the second peak of the SED is still under debate. In the leptonic model, the second peak results from the inverse Compton process between photons resulting from synchrotron radiation and the energetic electrons producing such photons (synchrotron self-Compton) or from interaction between energetic electrons in the jets with some external photons. In the hadronic model, the second peak in the SED is assumed to come from the radiation emitted by high energy protons (see Padovani et al. (2017) and references therein).

However, from our study covering more or less 12 years of observational data, we found that the SED of OJ 287 consists of at least three states: 1) Low power blazar SED which is dominated by the non-thermal processes from jets; 2) Low power blazar SED with significant thermal bremsstrahlung radiation; and 3) Low power blazar SED with shifting of high peak component.

5 Conclusion

We have studied optical–gamma ray data of OJ 287 covering more or less 12 years of observation. The following are the conclusions from our study.

- Optical and UV light curves of OJ 287 have quite similar pattern in long term but different profile in X-ray. While in gamma ray the light curve is quite stable except in around the brightening of 2016–2017 episode.
- There were two peaks of brightening detected in 2015–2017 which could not be clearly classified as the periodical outburst or not.
- We found different trends of the optical to X-ray spectra of OJ 287 and also with steep photon index during brightening of 2016–2017.
- The steeper the photon index of optical–UV spectra, the flatter the photon index of X-ray spectra become. While for gamma ray, photon index variability is quite stable except in the brightening of 2016–2017.

- The thermal bremsstrahlung before the brightening of 2015–2016 episode does seem contribute to the evolution of the SED.

Acknowledgements This work is supported by P3MI 2017 ITB Research Grant (KV, SF). This work made use of data supplied by the UK Swift Science Data Centre at the University of Leicester and the Fermi Science Support Center.

Publisher's Note Springer Nature remains neutral with regard to jurisdictional claims in published maps and institutional affiliations.

References

- Britzen, S., Fendt, C., Witzel, G., et al.: *Mon. Not. R. Astron. Soc.* **478**, 3199 (2018)
- Cardelli, J.A., Clayton, G.C., Mathis, J.S.: *Astrophys. J.* **345**, 245 (1989)
- Evans, P.A., Beardmore, A.P., Page, K.L., et al.: *Astron. Astrophys.* **469**, 379 (2007)
- Evans, P.A., Beardmore, A.P., Page, K.L., et al.: *Mon. Not. R. Astron. Soc.* **397**, 1177 (2009)
- Ghisellini, G., Righi, C., Costamante, L., et al.: *Mon. Not. R. Astron. Soc.* **469**, 255 (2017)
- Gupta, A.C., Agarwal, A., Mishra, A., et al.: *Mon. Not. R. Astron. Soc.* **465**, 4423 (2017)
- Ivanov, P.B., Igumenshchev, I.V., Novikov, I.D.: *Astrophys. J.* **507**, 131 (1998)
- Kalberla, P.M.W., Burton, W.B., Hartmann, D., et al.: *Astron. Astrophys.* **440**, 775 (2005)
- Kushwaha, P.: *Galaxies* **8**, 15 (2020)
- Kushwaha, P., Gupta, A.C., Wiita, P.J., et al.: *Mon. Not. R. Astron. Soc.* **479**, 1672 (2018)
- Laine, S., Dey, L., Valtonen, M., et al.: *Astrophys. J. Lett.* **894**, L1 (2020)
- Lehto, H.J., Valtonen, M.J.: *Astrophys. J.* **460**, 207 (1996)
- O'Brien, S.: (2017). ArXiv:e-prints, [arXiv:1708.02160](https://arxiv.org/abs/1708.02160)
- Padovani, P., Alexander, D.M., Assef, R.J., et al.: *Astron. Astrophys. Rev.* **25**, 2 (2017)
- Predehl, P., Schmitt, J.H.M.M.: *Astron. Astrophys.* **293**, 889 (1995)
- Siejkowski, H., Wierzecholska, A.: *Mon. Not. R. Astron. Soc.* **468**, 426 (2017)
- Sillanpää, A., Teerikorpi, P., Haarala, S., et al.: *Astron. Astrophys.* **147**, 67 (1985)
- Sillanpää, A., Haarala, S., Valtonen, M.J., et al.: *Astrophys. J.* **325**, 628 (1988)
- Sillanpää, A., Takalo, L.O., Pursimo, T., et al.: *Astron. Astrophys.* **305**, L17 (1996)
- Sillanpää, A., Takalo, L.O., Pursimo, T., et al.: *Astron. Astrophys.* **315**, L13 (1996)
- Sitko, M.L., Junkkarinen, V.T.: *Publ. Astron. Soc. Pac.* **97**, 1158 (1985)
- Valtonen, M.J.: *Astrophys. J.* **659**, 1074 (2007)
- Valtonen, M.J., Lehto, H.J.: *Astrophys. J. Lett.* **481**, L5 (1997)
- Valtonen, M., Sillanpää, A.: *Acta Polytech.* **51**, 76 (2011)
- Valtonen, M.J., Lehto, H.J., Sillanpää, A., et al.: *Astrophys. J.* **646**, 36 (2006a)
- Valtonen, M.J., Nilsson, K., Sillanpää, A., et al.: *Astrophys. J. Lett.* **643**, L9 (2006b)
- Valtonen, M.J., Ciprini, S., Lehto, H.J.: *Mon. Not. R. Astron. Soc.* **427**, 77 (2012)
- Valtonen, M.J., Zola, S., Ciprini, S., et al.: *Astrophys. J. Lett.* **819**, L37 (2016)
- Valtonen, M., Zola, S., Jermak, H., et al.: *Galaxies* **5**, 83 (2017)
- Vierdayanti, K., Done, C., Roberts, T.P., et al.: *Mon. Not. R. Astron. Soc.* **403**, 1206 (2010)